Journal of Photochemistry & Photobiology, B: Biology 234 (2022) 112533

Contents lists available at ScienceDirect

Journal of Photochemistry & Photobiology, B: Biology

journal homepage: www.elsevier.com/locate/jphotobiol

Refinement of water-filtered infrared A (wIRA) irradiations of *in vitro* acute and persistent chlamydial infections

Jasmin Kuratli [a,b,*], Cory Ann Leonard [a], Antonia Frohns [c], Robert Schoborg [d], Helmut Piazena [e], Nicole Borel [a]

[a] Institute of Veterinary Pathology (IVPZ) and Center for Applied Biotechnology and Molecular Medicine (CABMM), Vetsuisse Faculty, University of Zürich, Winterthurerstrasse 268, 8057 Zürich, Switzerland
[b] Graduate School for Cellular and Biomedical Sciences (GCB), University of Bern, Mittelstrasse 43, 3012 Bern, Switzerland
[c] Plant membrane biophysics, Technical University of Darmstadt, Schnittspahnstrasse 3, 64287 Darmstadt, Germany
[d] Department of Medical Education and Center for Infectious Disease, Inflammation and Immunity, Quillen College in Medicine, East Tennessee State University, PO Box 70582, Johnson City, TN 37614, USA
[e] Department of Anaesthesiology and Operative Intensive Care Medicine, Charité - Universitätsmedizin Berlin, Corporative Member of Freie Universität Berlin and Humboldt Universität zu Berlin, Berlin, Germany

ARTICLE INFO

Keywords:
Water-filtered infrared A (wIRA) and visible light (VIS) irradiation
Chlamydia trachomatis
Trachoma
Persistence
In vitro

ABSTRACT

Water-filtered infrared A (wIRA) alone or in combination with visible light (VIS) exerts anti-chlamydial effects *in vitro* and *in vivo* in acute infection models. However, it has remained unclear whether reduced irradiation duration and irradiance would still maintain anti-chlamydial efficacy. Furthermore, efficacy of this non-chemical treatment option against persistent (chronic) chlamydial infections has not been investigated to date. To address this knowledge gap, we evaluated 1) irradiation durations of 5, 15 or 30 min in genital and ocular *Chlamydia trachomatis* acute infection models, 2) irradiances of 100, 150 or 200 mW/cm^2 in the acute genital infection model and 3) anti-chlamydial activity of wIRA and VIS against *C. trachomatis* serovar B and E with amoxicillin (AMX)- or interferon γ (IFN-γ)-induced persistence. Reduction of irradiation duration reduced anti-chlamydial efficacy. Irradiances of 150 to 200 mW/cm^2, but not 100 mW/cm^2, induced anti-chlamydial effects. For persistent infections, wIRA and VIS irradiation showed robust anti-chlamydial activity independent of the infection status (persistent or recovering), persistence inducer (AMX or IFN-γ) or chlamydial strain (serovar B or E). This study clarifies the requirement of 30 min irradiation duration and 150 mW/cm^2 irradiance to induce significant anti-chlamydial effects *in vitro*, supports the use of irradiation in the wIRA and VIS spectrum as a promising non-chemical treatment for chlamydial infections and provides important information for follow-up *in vivo* studies. Notably, wIRA and VIS exert anti-chlamydial effects on persistent chlamydiae which are known to be refractory to antibiotic treatment.

1. Introduction

Chlamydia trachomatis (CT), an obligate intracellular bacterium, causes three major disease complexes in humans: Serovars A, Ba, B and C cause trachoma in developing nations, serovars D – K (genital serovars) represent the leading cause of bacterial sexually transmitted disease (STD) worldwide, and serovars L1 – L3 cause lymphogranuloma [1]. Trachoma, a neglected tropical disease, is characterized by repetitive infections with CT, beginning in early childhood. Subsequent progressive inflammatory processes in affected tissues lead to conjunctival scar formation, entropion (in-turned lid margin) and trichiasis (in-turned eyelashes) that can ultimately cause corneal opacity and irreversible blindness [2,3]. Ongoing elimination programs by the World Health Organization (WHO) aim to reduce trachomatous blindness by providing mass drug administration of antibiotics, surgery for individuals with ocular scar formation and hygiene improvements, summarized as the "SAFE strategy" [4]. Even though this strategy was partially successful, there are still 142 million people at risk of trachoma,

* Corresponding author at: Institute of Veterinary Pathology (IVPZ) and Center for Applied Biotechnology and Molecular Medicine (CABMM), Vetsuisse Faculty, University of Zürich, Winterthurerstrasse 268, 8057 Zürich, Switzerland.
E-mail addresses: jasmin.kuratli@uzh.ch (J. Kuratli), cory.leonard@uzh.ch (C.A. Leonard), schoborg@mail.etsu.edu (R. Schoborg), helmut.piazena@charite.de (H. Piazena), nicole.borel@uzh.ch (N. Borel).

https://doi.org/10.1016/j.jphotobiol.2022.112533
Received 30 March 2022; Received in revised form 23 June 2022; Accepted 20 July 2022
Available online 23 July 2022

and the goal of elimination by the year 2020 was not achieved [2,5,6]. While some authors are optimistic regarding elimination of trachoma on a population level in the next decade [2], other researchers highlight that remaining trachoma cases might still be relevant for public health considerations and are still problematic for the remaining high number of affected individuals in high population countries [7].

Challenges in the elimination of trachoma include the risk of progressive antibiotic resistance, re-emergence of trachoma after cessation of mass drug administration, ongoing difficulties of applying the SAFE strategy in conflict areas and difficulties in properly estimating trachoma prevalence in high population countries [2,5,7]. Even though homotypic CT resistance to azithromycin has not been reported to date, there are a remarkably high number of treatment failures (defined by CT positivity after antibiotic treatment) observed in trachoma patients and STD cases [2,8]. The reasons for these treatment failures are not entirely understood, but occurrence of heterotypic resistance caused by reduced growth rates of bacteria might be a relevant factor [2,8]. From *in vitro* studies, it is known that adverse growth conditions can induce *Chlamydia* to enter so-called chlamydial persistence or the chlamydial stress response, which is characterized by formation of enlarged chlamydial bodies (aberrant bodies [AB]), reduced chlamydial metabolism, reduced infectivity and reversibility of these characteristics upon removal of persistence inducers [9,10]. Persistent chlamydiae are refractory to antibiotic treatment *in vitro* [11] and *in vivo* [12]. Furthermore, there is evidence that persistent chlamydial forms might occur in natural infections *in vivo* (reviewed in [13]), leading to the conclusion that antibiotic treatment in these stages would not be successful. Though definitive proof of an important role for chlamydial persistence in human infections is still lacking [1,9,13], the strong evidence for its existence *in vivo*, in addition to the risk of escalating antibiotic resistance, indicates that exploration of non-antibiotic treatment options should be considered.

Water-filtered infrared A radiation (wIRA; wavelength 780–1400 nm, or 380–1400 nm when combined with visible light (VIS)) is a form of heat radiation characterized by good tissue penetration and mild superficial tissue heating [14–17]. As reviewed elsewhere, this radiation can promote anti-inflammatory effects and wound healing in acute and chronic wounds, and also has anti-bacterial properties [14,18,19]. We have demonstrated in previous studies that wIRA (and VIS) has anti-chlamydial effects in acute chlamydial infections *in vitro*. *In vivo* wIRA and VIS (595–1400 nm) treatment also reduces *Chlamydia*-induced inflammatory parameters in a guinea pig infection model without causing negative effects on ocular structures [18,20,21]. Therefore, wIRA radiation shows promise as a non-antibiotic treatment option for ocular chlamydial infections in humans [19], including trachoma and/or inclusion conjunctivitis caused by genital strains of CT [7,22–25]. wIRA and VIS radiation *in vitro* is effective against extracellular chlamydial developmental stages (elementary bodies, EBs) and against developing chlamydial inclusions containing dividing bacterial forms (reticulate bodies, RBs) in diverse cell culture models at irradiances of 200 mW/cm^2 or higher applied for at least 20 min [26–29]. The efficacy of shorter irradiation times or treatment of persistent chlamydial inclusions, however, has not been investigated so far. Such studies would provide insight into 1) the efficacy of wIRA and VIS in patients with chronic chlamydial disease and/or inflammatory ocular changes and the applicability of wIRA and VIS as non-antibiotic supplementary or alternative treatment option in such cases, 2) possible refinements of current treatment protocols to increase tolerability and ensure safety of wIRA treatment (as wIRA alone or in combination with VIS) and 3) the general working mechanism of wIRA and/or VIS against *Chlamydia*.

In this study, we therefore aimed to evaluate potential refinement of previously applied irradiation protocols *in vitro* by 1) determining whether single or triple short-duration irradiations of 5 or 15 min are effective against acute chlamydial infections and 2) whether the irradiation protocols proven effective in acute infection models are similarly effective in persistent infection models simulating chronic chlamydial disease in patients.

2. Material and Methods

2.1. Host Cells and Media

Homo sapiens cervix adenocarcinoma CCL-2 (HeLa, ATCC) and human conjunctival epithelial cells (HCjE), immortalized by hTERT transfection and kindly provided by Prof. Ilene Gipson (Schepens Eye Research Institute, Harvard Medical School, Boston), were used for this study. For propagation, cell lines were grown at 37 °C and 5% CO_2 in growth medium to a confluence of 80–100% before serial passaging. Composition of media is summarized in Table 1. HeLa infection medium was used for infecting cells, except for experiments with EB irradiation, where infections were done in growth medium (see 2.4.3.1.1). HCjE neutralization medium was used for thawing, serial passaging and inoculation of HCjE cells.

For experiments, cells were seeded at a density of 5×10^4 cells/well directly into wells or on glass coverslips (13 mm diameter, Thermo Fisher Scientific, Waltham, Massachusetts, USA) in 24-well plates (Techno Plastic Products AG (TPP), Trasadingen, Switzerland) and incubated for 24 h prior to infection.

2.2. Chlamydial Strains

Two strains of *Chlamydia trachomatis* were used in this study. The genital strain *Chlamydia trachomatis* Serovar E (CtE) (E/UW-5/) was originally obtained from S.P. Wang and C.-Cl. Kuo (University of Washington, Seattle, WA, USA) and used to infect HeLa cells, modeling a human genital infection. To simulate ocular infections, the ocular strain *Chlamydia trachomatis* Serovar B (CtB) (strain HAR-36, VR-573 ATCC, kindly provided by T. Barisani-Asenbauer, Vienna, Austria) was used in HCjE cells (irradiation duration experiments) or HeLa cells (persistence irradiation, see 2.4). Chlamydial stocks were grown in HeLa cells or rhesus monkey kidney cells (LLC-MK2, ATCC) as described previously [30].

2.3. Pharmaceutics

As a representative of the persistence inducing β-lactam antibiotics, we used amoxicillin trihydrate (AMX, CAS 61336–70-7, Sigma Aldrich).

Table 1
Composition of media used in this study.

Cell line	HeLa		HCjE	
Media names	Growth medium no Gentamycin (GnG)	Infection medium	Keratinocyte serum free medium (growth medium)	HCjE neutralization medium
Medium basis	MEM (Gibco, Life Technologies, Carlsbad, CA, United States)		Keratinocyte serum free medium (Gibco)	Dulbecco's Modified Eagle Medium/ Nutrient Mixture F-12 (DMEM/ F12, GIBCO)
Supplements	4 mM GlutaMAX-I (Gibco)		Bovine pituitary extract (final concentration 25 mg/ml; BPE, Gibco)	10% FCS (Bioconcept)
	1% MEM Non-Essential Amino Acids (MEM NEAA, 100×, Gibco)		Epidermal growth factor (final conc. 0.2 ng/ml; EGF, Gibco)	
	10% fetal calf serum (FCS, Bioconcept, Allschwil, Switzerland)	–	Calcium chloride 0.4 mM (Sigma-Aldrich, St. Louis, MO, USA)	

Stock solutions of 2 mg/ml AMX in sterile water were stored at −20 °C. Interferon-γ (IFN-γ) was obtained from Genscript Biotech, Oxford, UK via Lucerna-Chem AG, Luzern, Switzerland, dissolved in 0.1% Human Serum Albumin (HSA, Sigma Aldrich) in phosphate buffered saline (PBS; HSA/PBS) and stored at −80 °C at stock concentrations of 2000 U/µl (100 µg/ml, 20′000 U/µg). Tryptophan (TRP) from Thermo Scientific™ was dissolved in sterile water to 5 mg/ml stock concentration and stored at −20 °C.

2.4. Study Design

2.4.1. Determination of Doses for Persistence Induction

To determine the lowest persistence inducing dose of AMX and IFN-γ, dose curve experiments were performed. Typical features of chlamydial persistence include, amongst others: 1) AB formation and reduced infectivity upon exposure to persistence inducers and 2) the reversal of these changes, when the stress factor is removed (so-called recovery) [9]. Recovery times of 48 h for CtE and 60 h for CtB were chosen based on the observed growth characteristics of these strains and published literature [31]. We initially assessed persistence induction capacity of two different persistence inducers (AMX and IFN-γ) in the genital infection model using HeLa + CtE, followed by focused investigations for the ocular CtB strain as described in 2.4.1.1.

2.4.1.1. Amoxicillin. For the genital infection model, AMX stocks (2 mg/ml) were diluted to final concentrations of 0.001–10 µg/ml and the lowest persistence inducing concentration (0.1 µg/ml) was selected for subsequent persistence irradiation experiments with the CtE and CtB strain. Appropriate concentrations of sterile water (maximum 1% or lower) were added to growth media to serve as mock AMX exposure controls in all experiments with AMX.

2.4.1.2. Interferon-γ (IFN-γ). IFN-γ mediated chlamydial persistence in HeLa cells is caused by an indole-2,3-deoxygenase (IDO) mediated tryptophan depletion, which stresses the bacteria [32]. Dose curves of up to 3000 U/ml IFN-γ were used to determine the lowest persistence inducing dose (300 U/ml) of IFN-γ for use in subsequent irradiation experiments in the genital infection model; 0.1% HSA/PBS diluent in growth media was used for mock-exposed controls. We supplemented growth medium for recovery with TRP (110 µg/ml final TRP concentration; GnG TRP = 10 µg/ml), to reverse IFN-γ-mediated TRP depletion.

2.4.2. wIRA and VIS Irradiations

Irradiations were performed using two Hydrosun 750 wIRA radiators (Hydrosun GmbH, Müllheim, Germany) equipped with a 7 mm water-filter generating the spectrum covering VIS and wIRA (380–1400 nm) as depicted in Supplementary Fig. 1A. Spectral irradiance was measured as a function of wavelength with a double-monochromator spetroradiometer (type: SPECTRO 320D, Instrument systems, Munich, Germany) using spectral steps of 1 nm and spectral resolution of 1 nm. The spectroradiometer was calibrated by the manufacturer before use. It was equipped with an Ulbricht sphere as optical entrance window which was parallel and centered to the radiation output window of the radiator. Irradiances with different wavelength ranges are provided in Supplementary Fig. 1B. Total irradiance was set to 200 mW/cm^2±10% if not stated differently. To prevent excessive heating of monolayers during irradiation, plates were placed in a circulating water bath (SC100, Thermo Fisher Scientific) set to 37 °C like previously established and described elsewhere [26–28].

2.4.3. Infection and Irradiation Experiments (Fig. 1a - c)

2.4.3.1. Irradiation Duration Experiments (Fig. 1a)

2.4.3.1.1. EB-Irradiation. For EB-irradiation experiments, chlamydial stocks were thawed and diluted in HeLa growth medium (genital model) or neutralization medium (ocular model) to a calculated multiplicity of infection (MOI) of 1. These chlamydial suspensions were placed in 24 well plates (TPP) (1 ml/well), irradiated (or not) for 5, 15 or 30 min (see 2.4.2) and then transferred onto host cell monolayers. In addition to irradiations using 200 mW/cm^2, additional experiments using total irradiances of 300 mW/cm^2 were included for the genital infection model. Centrifuge-assisted infection was performed at 1000 g for 1 h at 25 °C, followed by removal of inoculum from infected monolayers and addition of fresh growth medium. Cultures were incubated for at least 43 (43–48) hours post infection (hpi) before collection of samples for experimental analysis (see 2.4.4).

2.4.3.1.2. Inclusion Irradiation. Cells were seeded and incubated for 24 h before the centrifuge-assisted chlamydial infection at an MOI of 1 was performed as described in 2.4.3.1.1. During the incubation of cultures for 43–48 hpi, irradiations were performed: cultures were either irradiated once for 5, 15 or 30 min at 24, 36 or 40 hpi (single irradiations) or irradiations were performed at all three time points for 5, 15 or 30 min, resulting in triple irradiations. The irradiation time points were based on our previous investigations [26–29]. A total irradiance of 200 mW/cm^2 was used for all experiments and the additional 300 mW/cm^2 was included for the genital infection model. At the end of the experiments, cultures were sampled for experimental analysis (see 2.4.4).

2.4.3.2. Comparison of Different Irradiances. The experimental setup was similar to inclusion irradiation experiments (see 2.4.3.1.2), with irradiations at 24, 36 and 40 hpi for 30 min, resulting in triple irradiations. Irradiatiors were set to total irradiances of 100, 150 or 200 mW/cm^2, to compare the effects of different stimuli. At 43 hpi, cultures were sampled for experimental analysis (see 2.4.4).

2.4.3.3. Persistence Irradiation Experiments (Fig. 1b and c). Seeding and incubation of HeLa cells was performed as described (see 2.4.3.1.2), followed by infection with either CtE (MOI = 1) or CtB (MOI = 10). After centrifugation, cultures were incubated with diluent alone (non-persistent, mock-exposed controls) or persistence inducer (0.1 µg/ml AMX or 300 U/ml IFN-γ) in growth medium for 43 h. During this incubation time, triple irradiations for 30 min at 24, 36 and 40 hpi were performed. We performed one additional experiment with a single irradiation for 30 min at 40 hpi in the AMX persistence model with HeLa + CtE. As depicted in Fig. 1c, persistence irradiation experiments were split into two sampling time points: one directly at 43 hpi allowing comparison of wIRA and VIS effects in persistence vs. control mock-exposed cultures (representing acute infections), and one after additional incubation for 48 h, the so-called recovery time. At this later time point, a comparison of wIRA and VIS effects in diluent-exposed cultures (mock, acute), continuously persistence inducer-exposed cultures (continued exposure, CE), and cultures recovering from persistence (recovery, rec) was possible. After the first sampling point, at 43 h, the remaining wells were washed twice with 1 ml/well infection medium. After this washing step, fresh media were added as follows: mock cultures were incubated in diluent-supplemented growth medium; continuously persistent cultures were incubated in AMX- or IFN-γ-supplemented growth medium (CE); and recovery conditions were incubated in diluent-supplemented growth medium (AMX rec) or TRP-supplemented (see 2.4.1.2), diluent-supplemented growth medium (IFN-γ rec), allowing *Chlamydia* to re-enter the regular developmental cycle. After this 48 h of additional incubation (or 60 h for CtB in HeLa), cultures were sampled for experimental analysis (see 2.4.4).

2.4.4. Experimental Analyses

2.4.4.1. Immunofluorescence Analysis (IFA). Monolayers grown on coverslips were fixed with ice cold methanol for 10 min, followed by processing for immunofluorescence assay (IFA) at room temperature. Blocking was done for 30 min using 1% bovine serum albumin (BSA)

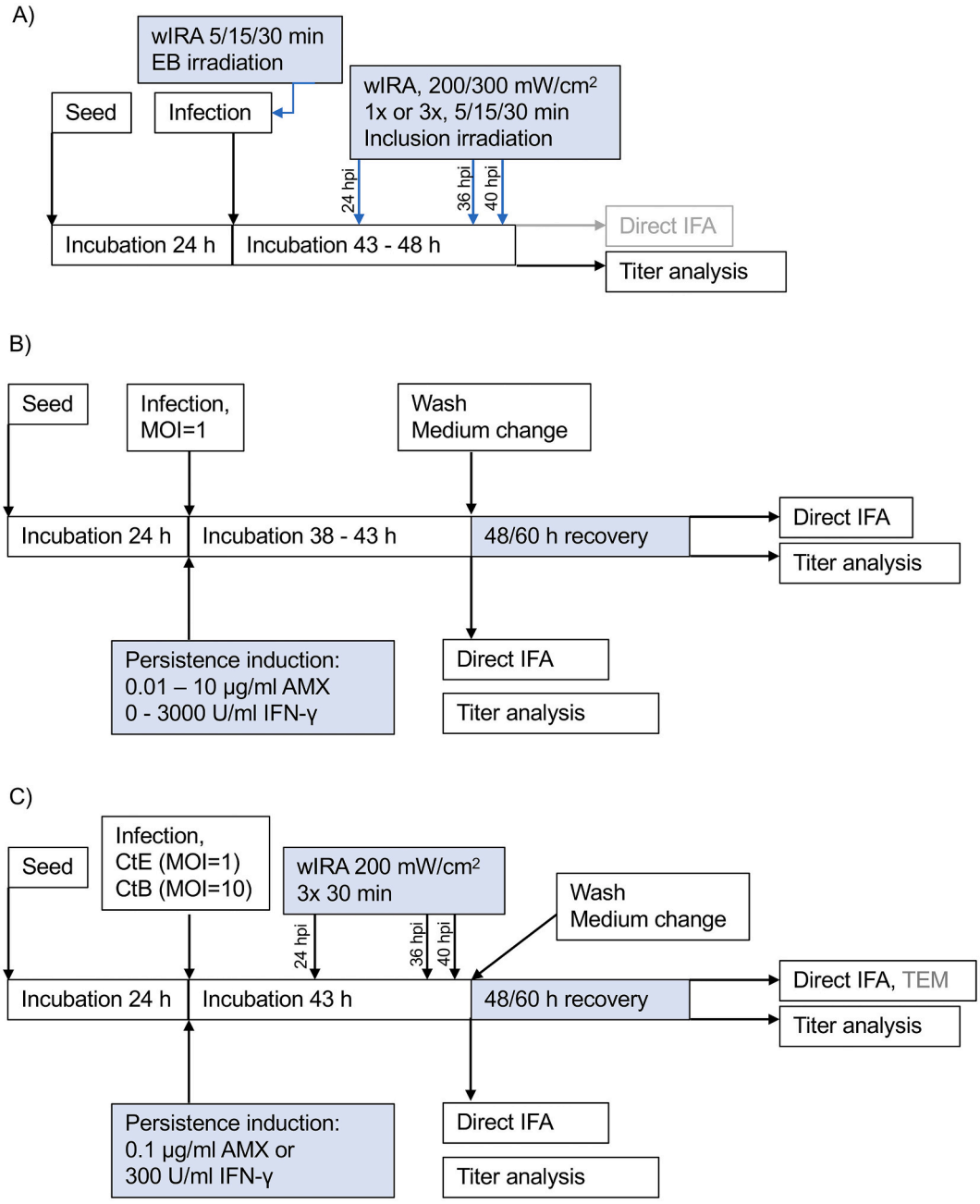

Fig. 1. Experimental settings: A) Schematic representation of irradiation duration experiments, in which either extracellular chlamydial bodies (EBs) were irradiated and used for infection, or cultures were infected first and developing chlamydial inclusions were wIRA and VIS irradiated as depicted. B) Experimental setting for irradiance determination for the two persistence inducers used in this study (AMX and IFN-γ). C) Experimental setting for irradiation of persistent (or control non-persistent) chlamydial cultures.

dissolved in PBS, followed by 1 h incubation in primary *Chlamydiaceae* family-specific mouse monoclonal antibody (1:300 in 1% BSA, LPS, Clone, ACl-P, Progen, Heidelberg, Germany). Coverslips were washed three times with PBS to remove unbound antibody, followed by 1 h incubation in secondary antibody (Alexa Fluor 488-goat anti-mouse antibody, 1:750 in 1% BSA, Thermo Fisher Scientific) with 4′,6-Diamidin-2′-phenylindoldihydrochlorid (DAPI, 1 µg/mL final concentration, Molecular Probes, Eugene, OR, USA) included to stain bacterial and host cell DNA. Coverslips were washed three times with PBS after the final incubation and mounted on glass slides using FluoreGuard Mounting medium (Hard Set, ScyTek Laboratories Inc., Logan, UT, USA). Slides were examined on a DMLB fluorescence microscope (Leica Microsystems, Wetzlar, Germany).

2.4.4.2. Direct IFA Analysis of Inclusion Size/Morphology and Percent Infection. For each experimental condition, one well with coverslip was included to analyze effects of treatments on *Chlamydia*; for persistence experiments, the well/coverslip from a single representative experiment of three replicate experiments was selected. Coverslips processed for IFA (see 2.4.4.1) were analyzed for effects on 1) inclusion size, 2) inclusion morphology and 3) percent of host cells infected (% infection). Inclusion size analysis was performed by randomly selecting 50 inclusions on the coverslip at 400× magnification. Inclusion area was determined with the BonTec measuring and archiving software (BonTec, Bonn, Germany) and means and standard deviations (sd) were calculated with Microsoft Excel (Microsoft, Redmond, WA, USA). Percent infection was determined by counting inclusions (green fluorescence channel) and host cell nuclei (blue fluorescence channel) in 30 randomly selected, reticle-

delimited fields at 1000× magnification with oil immersion. For each field, % infection was determined by dividing the number of inclusion by the number of host cell nuclei and multiplying by 100. Percent infection for 30 randomly selected fields was averaged for each coverslip. Inclusion morphology was documented by taking images of representative inclusions at 1000× magnification.

2.4.4.3. Chlamydial Infectivity Analysis by Sub-Passage Titration Analysis. Chlamydial infectivity (titer) was determined by sub-passage titration analysis as previously described [33]. For each experimental condition, duplicate wells for titer were included. At titer sample collection, monolayers were collected either by scraping them directly into the existing growth medium (dose determination and persistence experiments) or by removal of growth medium followed by scraping into freshly added infection or neutralization medium (irradiation duration experiments) and samples were stored at −80 °C until analysis. For the subsequent titers, confluent HeLa monolayers were seeded in 24 well plates with coverslips (Thermo Fisher Scientific), incubated for 24 h and monolayers were infected by serial dilutions of thawed titer samples in HeLa infection medium, followed by centrifugation for 1 h at 1000 *g* and 25 °C. After centrifugation, medium was either directly (no wash step) replaced by HeLa growth medium supplemented with 1 μg/ml cycloheximide (for samples from irradiation duration experiments), or monolayers were washed once with 1 ml/well HeLa infection medium to remove residual persistence inducers (for samples from dose determination and persistence experiments) before adding the growth medium supplemented with 1 μg/ml cycloheximide. Cultures were incubated about 40 h, then fixed with methanol and processed for IFA (see 2.4.4.1). Number of chlamydial inclusions per field in 30 randomly selected, reticle-delimited fields (high infectivity) or on the whole coverslip (low infectivity) were counted at a 200× or 400× magnification and IFU/ml values were calculated for each sample using Microsoft Excel as described previously [33].

2.4.4.4. Transmission Electron Microscopy. In addition to inclusion morphology as determined by IFA, we assessed ultrastructural morphology by transmission electron microscopy (TEM) evaluation of selected experimental conditions, as described previously [34,35].

2.5. Data Collection and Statistical Analysis

Except for pharmaceutics and irradiation dose curves, all experiments were performed three times, independently. For each experiment, three wells per condition were included, one of which (with coverslip) served as direct IFA sample (see 2.4.4.2) and two of which (no coverslip) were used for sub-passage titer analysis (see 2.4.4.3). In figures, infectivity IFU/ml values of corresponding non-irradiated controls (located on the same plate as the irradiated samples) were set to 100%, whilst infectivity of matched irradiated samples were expressed as % of corresponding control±SD. Short labels of figure axes were chosen to ensure readability. Therefore, irradiated conditions in figures are termed "wIRA", but cover the spectrum of 380–1400 nm (wIRA and VIS).

Statistical analyses were performed in R[1] using calculated IFU/ml values (infectivity analysis) or nuclei counts as response variables. These were evaluated for (normal) distribution graphically and by performing shapiro wilk tests. Depending on the distribution of the response variable, number of experimental groups and number of explanatory variables, different statistical analyses were performed. Two experimental groups were compared using student's *t*-test or a non-parametric Wilcoxon Rank Sum test. Three or more experimental groups with one explanatory variable were compared using a one-way ANOVA or a generalized linear model (GLM). Three or more experimental groups with two explanatory variables (e.g. infection status (persistence or mock at 43 h and 91 h) and irradiation status (irradiated (wIRA) vs. ctrl) were analyzed using two-way ANOVA or GLM. For each dataset investigated, the best fitting model was chosen by comparing model fits using the Akaike information criterion (AIC function) and running DHARMa model diagnostics (DHARMa package). Analyses were followed by Tukey post hoc test (multicomp package [36]) for multiple comparisons of explanatory variables. Separate non-irradiated controls for each irradiation protocol (e.g. single irradiations at 24 hpi vs. 40 hpi) were located on the same plate for technical reasons, generating multiple control groups per irradiation experiment and increasing the number of comparisons in these datasets. To avoid irrelevant comparisons, a two-step approach was chosen for these datasets. Initially, statistical analyses as described above were performed to compare the multiple control groups originating from a single experiment. If these did not differ, they were summarized as one control group and compared to different irradiation groups in the explanatory variable, followed by statistical analysis using the best fitting model.

3. Results

3.1. EB Irradiations Shorter than 30 min are Not Sufficient to Reduce Chlamydial Infectivity (Figs. 1a, 2)

To test the effects of short(er) irradiation times on extracellular, infectious chlamydial stages, we irradiated CtE EBs for 5, 15 or 30 min

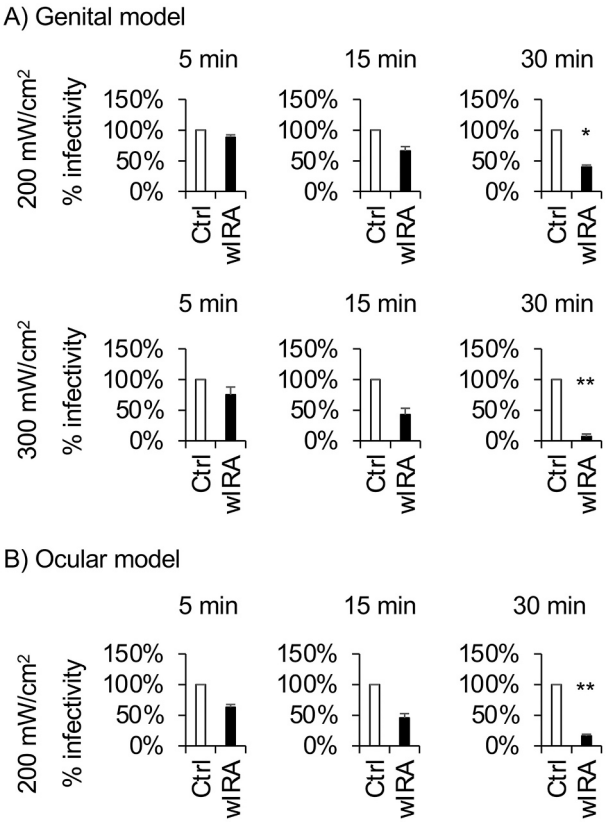

Fig. 2. wIRA and VIS effects on chlamydial infectivity, irradiation of extracellular EBs prior to infection: A) Genital infection model using HeLa cells and *Chlamydia trachomatis* serovar E (CtE). B) Ocular model with HCjE cells and *Chlamydia trachomatis* serovar B (CtB). Chlamydial infectivity (IFU/ml) in non-irradiated controls (Ctrl) was set to 100% and irradiated (wIRA) infectivity was expressed as % of the corresponding control. Bars show mean % infectivity ± SD from three independent experiments. Statistical analysis was done using Wilcoxon test to compare the Ctrl and wIRA IFU/ml data (* $p < 0.05$, ** $p < 0.01$).

[1] The cran project https://www.r-project.org

using two different irradiances (200 mW/cm^2 or 300 mW/cm^2) before using the EBs to infect HeLa cells (genital model). We did not observe significant reduction in chlamydial infectivity after 5 or 15 min irradiations with either irradiance (Fig. 2A). In contrast, an irradiation duration of 30 min reduced chlamydial infectivity to 40 ± 2.87% ($p < 0.05$) for 200 mW/cm^2 and to 7.00 ± 4.13% ($p < 0.01$) for 300 mW/cm^2 compared to the controls (Fig. 2A). However, the strong decrease in chlamydial infectivity for the higher irradiation dose was accompanied by cytotoxicity: a significant reduction of nuclei counts to 21.17 ± 5.95 nuclei/field in wIRA and VIS treated conditions, compared to 26.03 ± 2.70 nuclei/field in controls, was observed at 300 mW/cm^2 ($p < 0.05$; Supplementary Fig. 2). At 200 mW/cm^2, nuclei numbers did not differ between the irradiated cultures (23.4 ± 3.21 nuclei/field) and the controls (24.7 ± 2.91 nuclei/field) (Supplementary Fig. 2).

Due to the cell toxicity, CtB EBs (ocular model, HCjE cells) were only irradiated with 200 mW/cm^2 and loss of nuclei was prevented (data not shown). In the ocular model, irradiation durations of 30 min reduced infectivity to 16.18 ± 2.83% of the controls (Fig. 2B, $p < 0.01$) while 5 min and 15 min of irradiation duration did not lead to a significant decrease of chlamydial infectivity (63.08 ± 4.54% and 45.71 ± 6.93%, respectively). We thus conclude that irradiation durations longer than 15 min are needed to induce a statistically significant reduction of chlamydial infectivity.

3.2. Reduction of Chlamydial Infectivity Upon Irradiation of Developing Inclusions is Dependent on Irradiation Duration and Timing (Figs. 1a, 3)

Based on the observations that infectivity of extracellular chlamydial EB was only significantly reduced upon 30 min of irradiation, we aimed to investigate how shorter irradiation durations would impact infectivity of developing chlamydial inclusions containing reticulate bodies (RBs) and elementary bodies (EBs). Independent of the model used, 5 min of wIRA and VIS irradiation (200 or 300 mW/cm^2) was not sufficient to reduce chlamydial infectivity, either as single irradiation, or as triple irradiation (Fig. 3). For 15 min of irradiation at 200 mW/cm^2, triple irradiations reduced chlamydial infectivity to 57.0 ± 18.82% ($p < 0.01$) in the genital model and 33.64 ± 29.18% ($p < 0.001$) in the ocular model, while single irradiations at 24, 36 or 40 hpi were not sufficient to reach significant reduction of infectivity in either of the models. In the ocular model, however, significant differences in infectivity upon triple and single irradiations of infected cells were observed (Fig. 3), which was not the case for the genital infection model at 200 mW/cm^2.

In the genital model, a single irradiation for 15 min with the higher irradiance of 300 mW/cm^2 reduced chlamydial infectivity to 53.66 ± 1.30% at 24 hpi, compared to the control ($p < 0.05$), while infectivity for irradiation at 36 hpi (63.07 ± 5.47%) or 40 hpi (83.01 ± 11.90%) was not significantly reduced (Fig. 3A). This might indicate that irradiation during an earlier time point of the infectious cycle (24 vs. 36 or 40 hpi)

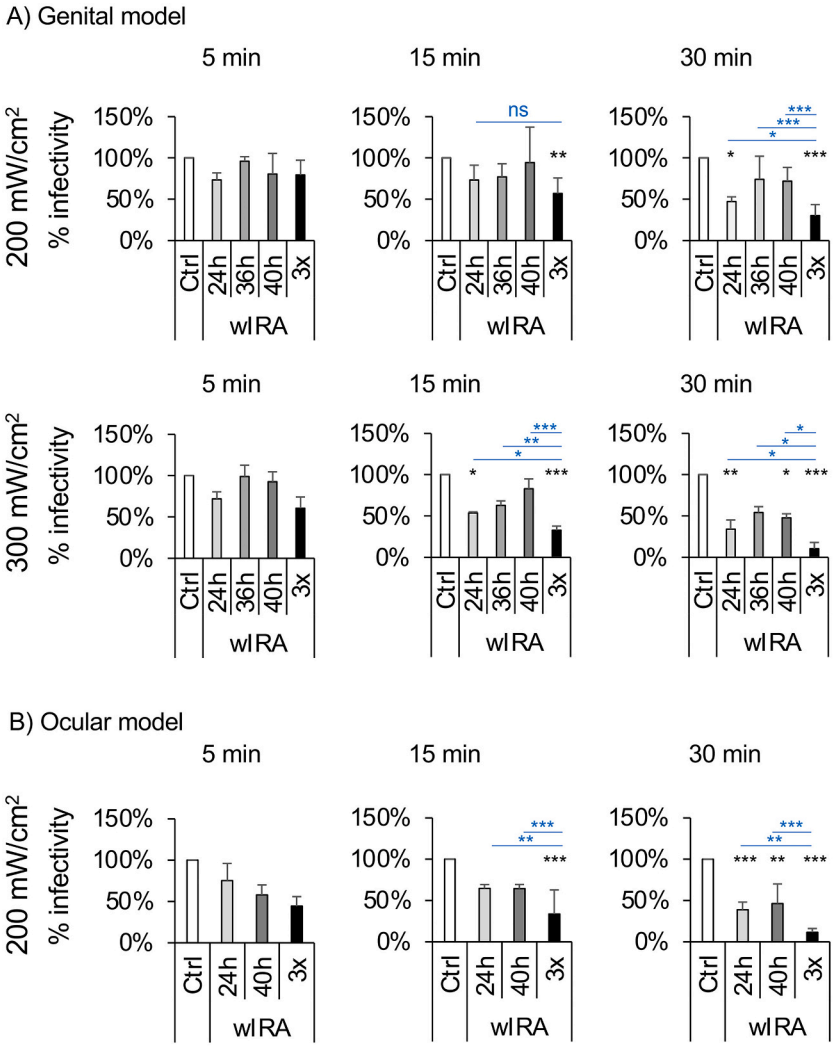

Fig. 3. Effects of wIRA and VIS irradiation on chlamydial infectivity, irradiation of developing chlamydial inclusions: A) Genital infection model using HeLa cells and CtE. B) Ocular model with HCjE cells and CtB. Chlamydial infectivity (IFU/ml) in non-irradiated controls (Ctrl) was set to 100% and irradiated (termed "wIRA"in the figure axes) infectivity was expressed as % of the corresponding control. Bars show the mean % infectivity ± SD from three independent experiments. Black asterisks indicate significant differences for Ctrl vs. irradiated samples, while blue asterisks (or ns) represent differences between irradiation protocols (e.g. single irradiation with wIRA and VIS vs. 3× irradiations). Statistical analyses were performed using generalized linear models (GLM) with Tukey post hoc on IFU/ml raw data with summarized controls (see 2.5) (* $p < 0.05$, ** $p < 0.01$, *** $p < 0.001$, ns = not significant). (For interpretation of the references to colour in this figure legend, the reader is referred to the web version of this article.)

could be relevant for chlamydial susceptibility to wIRA and VIS effects. Triple irradiations for 15 min reduced infectivity to 32.82 ± 4.98%, which differed significantly from both the control infectivity values and the infectivity values for single irradiations, meaning that repetitive irradiation treatments are more effective than single irradiations in this setting.

For 30 min irradiations, infectivity upon triple irradiation differed significantly from infectivity upon single irradiation in both cell culture models, an effect observed for both irradiances evaluated in the genital model (Fig. 3). Triple irradiations with 200 mW/cm^2 for 30 min reduced chlamydial infectivity significantly ($p < 0.001$) to 30.22 ± 13.35% of control values in the genital model and to 11.67 ± 4.46% of control values in the ocular model, while triple irradiations with 300 mW/cm^2 reduced infectivity to 10.42 ± 7.53% in the genital model (Fig. 3). Interestingly, the infectivity after single irradiations was only significantly reduced when irradiations were performed at 24 hpi or 40 hpi, but not at 36 hpi, in the genital infection model (Fig. 3), again pointing towards a variable susceptibility of *Chlamydia* to wIRA and VIS effects during the course of infection.

We conclude that multiple irradiation treatments are more effective than single treatments and that sufficient irradiation duration is required to significantly reduce chlamydial infectivity. Depending on the irradiance, the threshold irradiation duration to reach a significant anti-chlamydial effect is between 15 and 30 min (300 mW/cm^2, 1 × 15 min at 24 hpi or 1 × 30 min at 24 or 40 hpi) or between 30 and 45 min (200 mW/cm^2, 1 × 30 min at 24 or 40 hpi or 3 × 15 min at 24/36/40 hpi).

3.3. wIRA and VIS Anti-Chlamydial Effects are Independent of Developmental Stage (Acute Versus Amoxicillin-Induced Persistent Infection) (Fig. 4, Table 2)

We evaluated the efficacy of a single 30 min irradiation at 40 hpi in persistent vs. acute infections. We did not find a statistically significant reduction of chlamydial infectivity in this setting (data not shown). Therefore, we focused on triple irradiations for 30 min at 200 mW/cm^2 (at 24, 36 and 40 hpi) as depicted in Fig. 1C. As expected, amoxicillin exposure significantly ($p < 0.001$) reduced chlamydial infectivity compared to mock-exposed cultures (ie non-persistent) (Table 2). When amoxicillin was removed, and cultures were allowed to recover from persistence (AMX rec), infectivity was restored, meaning that IFU/ml levels differed significantly from AMX CE ($p < 0.001$) infectivity, but not from mock-exposed infectivity ($p = 0.976$).

Due to the high standard deviation in our experiments, we displayed infectivity as percent infection of corresponding (non-irradiated) controls, to better visualize differences between irradiated and non-irradiated conditions (Fig. 4B, Table 2). For statistical analysis, however, we entered raw IFU/ml data into a GLM (see material and methods, section 2.5), in which wIRA and VIS effects were highly significant amongst all groups ($p < 0.001$) and no interactions between the explanatory variables were detected. Interestingly, we observed reduced chlamydial infectivity after irradiation in all experimental conditions, even in persistent cultures and in formerly persistent, recovering cultures (AMX rec) (Table 2; Fig. 4B). Immunofluorescence analysis of amoxicillin-exposed vs. mock-exposed groups, for irradiated vs. control non-irradiated groups, did not show many differences in inclusion morphology (Fig. 4C). Therefore, we assessed chlamydial inclusion sizes, nuclei numbers and percent infection in only one of three independent experimental replicates (Supplementary Fig. 3A). Even though we did not observe obvious difference between irradiated and non-irradiated conditions in mock-exposed cultures and inclusions upon continuous exposure to AMX, it appeared as if wIRA and VIS irradiation impacted morphology in AMX rec conditions: while non-irradiated controls showed an almost normal morphology (granular inclusions with very few ABs), irradiated inclusions still resembled the aberrant morphology observed in continued exposure cultures. This was further investigated by TEM, visualizing the ultrastructural morphology of these inclusions in HeLa cells at 91 hpi (Fig. 4D). Mock-exposed cultures mainly contained regular chlamydial inclusions containing EBs (small, electron dense) or RBs (slightly larger, less electron dense). We also observed occasional aberrant bodies in mock-exposed cultures (characterized by less electron dense particles with >2 μm diameter) independent of the irradiation status. While continuously amoxicillin-exposed (AMX CE), but non-irradiated inclusions contained ABs, the corresponding irradiated inclusions seemed to be emptier and/or included only a few ABs that were irregularly shaped. In amoxicillin recovery conditions (AMX rec), it was difficult to detect chlamydial inclusions at all (only few inclusions present, independent of irradiation group), but the few documented inclusions showed clear differences in morphology between control and irradiated groups: while in the non-irradiated control most inclusions contained regular chlamydial bodies, or a mixture of aberrant and reticulate bodies, indicating recovery from persistence, wIRA and VIS-exposed inclusions looked empty or contained material that could not be identified as chlamydial bodies (Fig. 4D). We summarize that wIRA and VIS irradiation reduced infectivity in aberrant chlamydial forms and that this reduction was associated with morphological and ultrastructural changes of inclusions and chlamydial particles.

3.4. wIRA and VIS Anti-Chlamydial Effects are Independent of the Persistence Model (Interferon-γ Persistence, Fig. 5, Table 3)

IFN-γ exposure significantly ($p < 0.001$) reduced chlamydial infectivity, independent of irradiation, at 43 hpi and 91 hpi (Table 3). When recovery in tryptophan (TRP)-supplemented growth medium was induced (to help replenish IFN-γ-depleted TRP), infectivity of samples was restored as expected (Fig. 5A, Table 3). wIRA and VIS significantly reduced infectivity in all conditions compared to corresponding non-irradiated controls ($p < 0.001$ in a GLM). Similar to cultures recovering from amoxicillin persistence, wIRA and VIS effects remained even after additional 48 h of recovery with TRP supplementation (Fig. 5B, Table 3).

Immunofluorescence analysis revealed similar inclusion morphology for non-irradiated and irradiated cultures. IFN-γ-exposure only mildly impacted chlamydial morphology at 43 hpi or upon recovery after removeal of IFN-γ, while continuously exposed cultures (IFN CE) at 91 hpi showed strong reduction in chlamydial inclusion size and enlarged structures indicative of aberrant bodies were visible inside the inclusions (Fig. 5C). In ultrastructural analysis, we observed the expected inclusion morphology for non-irradiated inclusions in mock-exposed and recovery conditions, but it was difficult to detect the small, atypical inclusions in the (non-irradiated) IFN CE group. However, we observed rare inclusions in the irradiated IFN CE group with aberrant morphology of chlamydial bodies. In contrast to the AMX persistence model, where the IFA and TEM morphology correspond well to the infectivity results, we did not find a similar correlation between reduced infectivity and inclusion morphology in the IFN model. This led us to hypothesize that irradiated inclusions recovering from IFN either contain less EBs but more RBs (Fig. 5D), or have similar numbers of normal-appearing but less infectious EBs, compared to the recovering non-irradiated controls. However, we did not follow-up with further analysis of inclusion bacterial form composition vs. infectivity in this study. Inclusion size measurements, nuclei counts and percent infection analysis of one representative experiment of three independent experiments are depicted in Supplementary Fig. 3B. We observed a strong reduction in inclusion size and percent infection for the IFN-γ-exposed group at 91 h of continued exposure. Recovery with TRP supplementation reversed this effect and led to increased inclusion size. In general, inclusion sizes for wIRA and VIS treated conditions seemed smaller, but since this data originates from a single experiment, we did not perform statistical

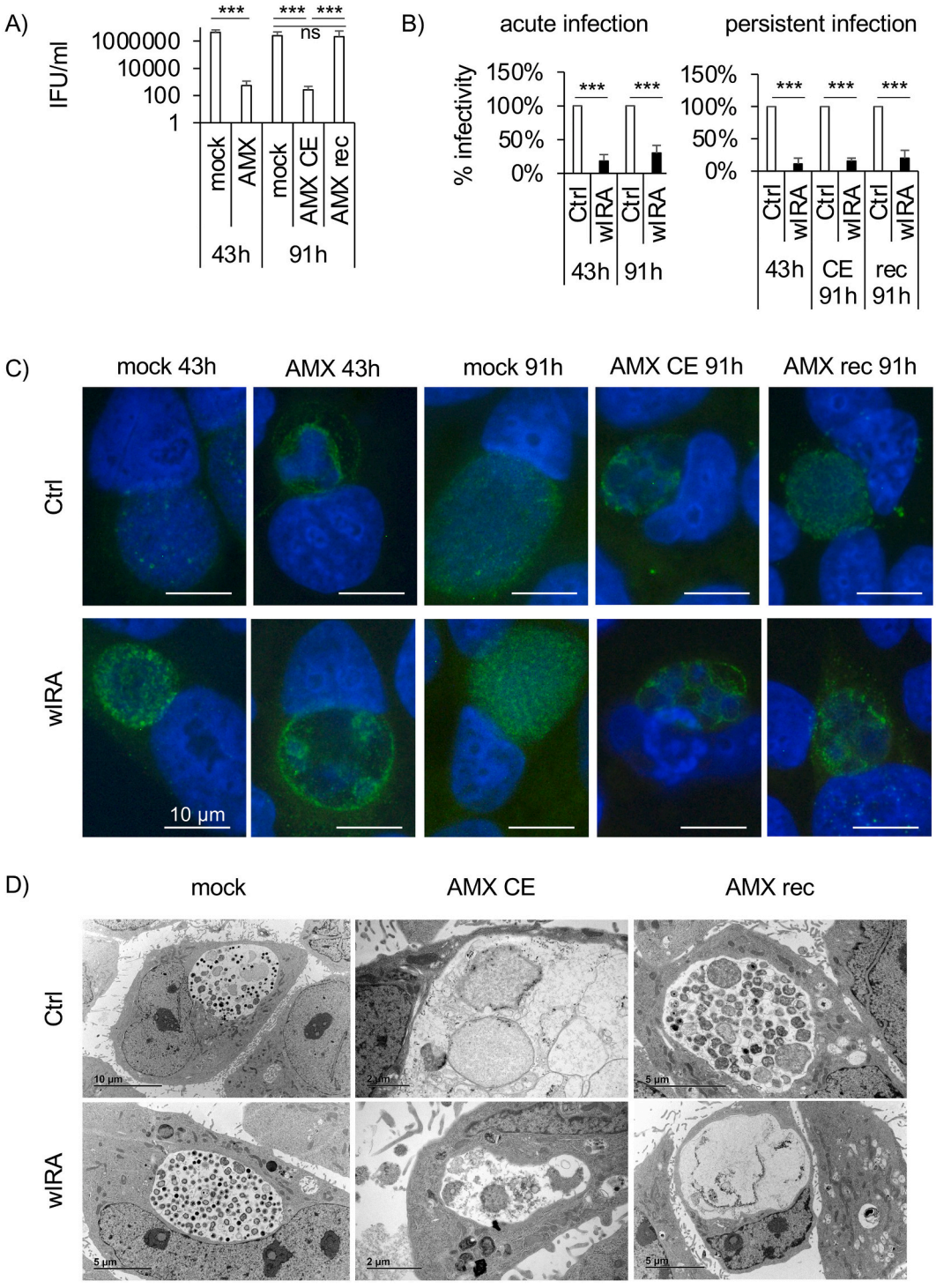

Fig. 4. Effects of AMX and/or irradiation on chlamydial infectivity and morphology in a genital infection model: A) infectivity (IFU/ml) in non-irradiated conditions, exposed (AMX) or not (mock) to amoxicillin, and B) infectivity in non-irradiated controls (Ctrl) (set to 100%) vs. irradiated ("wIRA") conditions (expressed as % of control) for acute infection (exposed to diluent only, mock) and persistent infection (exposed to AMX). C) Representative immunofluorescence images of inclusions. D) Representative transmission electron microscopy images of inclusion ultrastructure at 91 hpi. For all plots, the bars represent values from three independent experiments ± SD. Statistical analysis was performed using a generalized linear model with IFU/ml raw data as response variables and experimental group (43 h mock vs. AMX, 91 h mock vs. AMX CE vs. AMX rec) and irradiation status (Ctrl vs. irradiation ("wIRA")) as explanatory factors. No interaction was detected for the applied model. Post hoc analysis was done with the Tukey test. *** $p < 0.001$.

analysis. In the nuclei count, we observed some toxicity (nuclei loss) of IFN-γ on HeLa cells, without obvious irradiation-dependent exacerbation, which was partially reversible over the 48 h of IFN-γ free recovery. Overall, we observed variable effects of wIRA and VIS irradiation on inclusion morphology in the two persistence models, but the reduction of chlamydial infectivity, even upon recovery, was consistently observed in both models of chlamydial persistence, indicating a reproducible, limiting effect of irradiation on chlamydial development in this stage of infection.

Table 2
Amoxicillin and irradiation effects on chlamydial infectivity in the genital infection model with or without amoxicillin-induced persistence.

Sampling timepoint	Condition	Control only IFU/ml; Fig. 4A – AMX effect	% of control after irradiation; Fig. 4B – irradiation effect
43 h	Mock	$4.16 \times 10^6 \pm 2.37 \times 10^6$	18.50 ± 9.33
	AMX	$5.46 \times 10^2 \pm 5.92 \times 10^2$	11.28 ± 8.87
91 h	Mock	$2.53 \times 10^6 \pm 2.07 \times 10^6$	29.87 ± 11.53
	AMX CE	$2.65 \times 10^2 \pm 2.04 \times 10^2$	15.38 ± 4.77
	AMX rec	$2.08 \times 10^6 \pm 3.37 \times 10^6$	19.79 ± 12.44

3.5. wIRA and VIS Anti-Chlamydial Effects Against Persistent Chlamydia are Independent of the Chlamydial Strain (Fig. 6)

Irradiation-dependent anti-chlamydial effects against persistent CtE were consistent across both amoxicillin- and IFN-γ-induced persistence. We sought to determine if the observed anti-chlamydial effects are reproducible in an ocular chlamydial strain, CtB. Since ocular chlamydial strains are typically less infectious than genital strains, and given very low residual infectivity in CtB after AMX-exposure, we used an MOI of 10 in these experiments. The persistence-inducing effects of amoxicillin and the corresponding irradiation effect on CtB infectivity are depicted in Table 4. Interestingly, recovery of 60 h after amoxicillin removal allowed significant increase in chlamydial infectivity ($p < 0.001$ compared to AMX CE). But, in contrast to the results observed for CtE infectivity upon recovery from amoxicillin- or IFN-γ-induced persistence (Figs. 4A, 5A), infectivity in the recovering CtB group remained significantly less than than of the mock-exposed control ($p < 0.001$), leading us to conclude that the original level of infectivity was not regained upon recovery (Fig. 6A, Table 4). wIRA and VIS exposure reduced the chlamydial infectivity of all persistent cultures, including recovery conditions (Fig. 6B, Table 4).

For mock-exposed cultures (with non-persistent chlamydial infection), however, we observed reductions of CtB infectivity at 43 hpi, while at 91 hpi we observed an irradiation-associated increase in infectivity compared to the non-irradiated control in one of three experimental replicates, resulting in a mean chlamydial infectivity of 68.54 ± 46.83% of the corresponding control value over all experimental replicates (Table 4). In the GLM, this variation in wIRA and VIS effects in the mock-exposed acute infection was detected as a significant interaction for the group variable (91 h, recovery) and irradiation variable (indicated by green line, Fig. 6B). We therefore ran an interaction model for this dataset, in which the overall wIRA and VIS effect was significant with $p < 0.05$. We conclude that anti-chlamydial effects of wIRA and VIS can be reproduced in two clinically relevant *Chlamydia trachomatis* strains and two different models of chlamydial persistence.

3.6. Triple Irradiation Reduces Infectivity of Acute Infections at 200 and 150, but not at 100 mW/cm^2

In our investigation of potential refinement of the therapeutic applications of wIRA and VIS, we were interested in evaluating the anti-chlamydial efficacy of irradiation protocols that may cause less heating of patients' (ocular) tissues. As shorter-duration irradiations failed to reduce chlamydial infectivity significantly, we wanted to determine if anti-chlamydial effects could still be achieved with reduced irradiances. We therefore used the triple irradiation protocol with 30 min irradiations at 24, 36 and 40 hpi in the genital infection model to compare the effect of irradiances of 200, 150 or 100 mW/cm^2. Chlamydial infectivity in irradiated groups was 35.56 ± 12.40%, 33.74 ± 15.89% and 45.21 ± 14.99% compared to corresponding controls at 200, 150 and 100 mW/cm^2, respectively (Supplementary Fig. 4). These effects were significant in a GLM with Gamma errors for irradiances of 200 and 150 mW/cm^2 ($p < 0.001$), but not for 100 mW/cm^2 ($p > 0.05$); infectivity was equivalent amongst the different irradiances. We therefore conclude that similar anti-chlamydial effects against acute infections may be achieved for triple irradiation, even when reducing the irradiance to 150 mW/cm^2 as an alternative to 200 mW/cm^2.

4. Discussion

Anti-chlamydial effects of wIRA (and VIS) have been reported for various cell culture models (reviewed in [18,19]) and *in vivo* in a guinea-pig inclusion conjunctivitis infection model [20]. Though no detrimental effects of this irradiation on host cells or induction of heat-responsive proteins have been reported so far [21,26,28], investigation of potential refinement of wIRA irradiation protocols is useful to 1) assess the efficacy of adapted treatment regimens and 2) gain information about the nature and mechanisms of anti-chlamydial wIRA and VIS effects.

4.1. Short-Duration Irradiations Inform Thresholds for Irradiance and Irradiation Duration

In this study, we report that irradiations of 5 or 15 min duration are not sufficient to cause significant reduction of chlamydial infectivity *in vitro*, while we confirm previous results of effective anti-chlamydial treatments at longer or repetitive irradiations [20,26–29]. Interestingly, we observed irradiation induced toxicity for HeLa cells in the 30 min EB irradiation experiments at 300 mW/cm^2 of total irradiance despite the short inoculation of cells in the irradiated medium. As the used irradiance was higher than the needed level for anti-chlamydial efficacy and we did not observe toxicity at 200 mW/cm^2, we did not further follow-up this result. However, published literature indicates that irradiation of culture medium by VIS can induce the production of cytotoxic agents depending on the medium composition [37], which might explain our observation. Our data point towards thresholds of wIRA and VIS irradiation efficacy at 150–200 mW/cm^2 for around 30 min (e.g. single irradiation for 30 min) or 45 min (repetitive irradiations with a total irradiation time of 45 min, e.g. 3 × 15 min). The to date limited knowledge about the underlying working mechanisms of wIRA and VIS anti-chlamydial effects (see also sections 4.4 and 4.6), however, do not allow application of the Bunsen-Roscoe law of reciprocity for this irradiation. This law states that observed irradiation effects in a biological system are directly proportional to the total irradiation dose used, independent of irradiance, duration or modality of administration (meaning that there should be the same effect with shorter irradiations at higher irradiances compared to longer exposures with lower irradiances) [38]. It is therefore too early to directly compare the total irradiation dose of our irradiation protocols to those achieved with other irradiation techniques like e.g. antimicrobial photodynamic therapies (aPDT), where photosensitizing agents are combined with suitable light sources to achieve antimicrobial biological effects (reviewed in [39]). Further research on the linearity of wIRA and VIS irradiation effects and the applicability of the Bunsen Roscoe law should be performed in the future to close these remaining knowledge gaps.

4.2. Evidence for Differential Susceptibility of Chlamydial Inclusions During Development

While single irradiations for 30 min were effective at the 24 and 40 hpi timepoints, confirming similar previous results for single irradiations of 20 or 30 min at 40 hpi [26–28], a single 30 min irradiation at 36 hpi in the genital infection model did not significantly reduce chlamydial infectivity. Currently, we can only speculate on potential

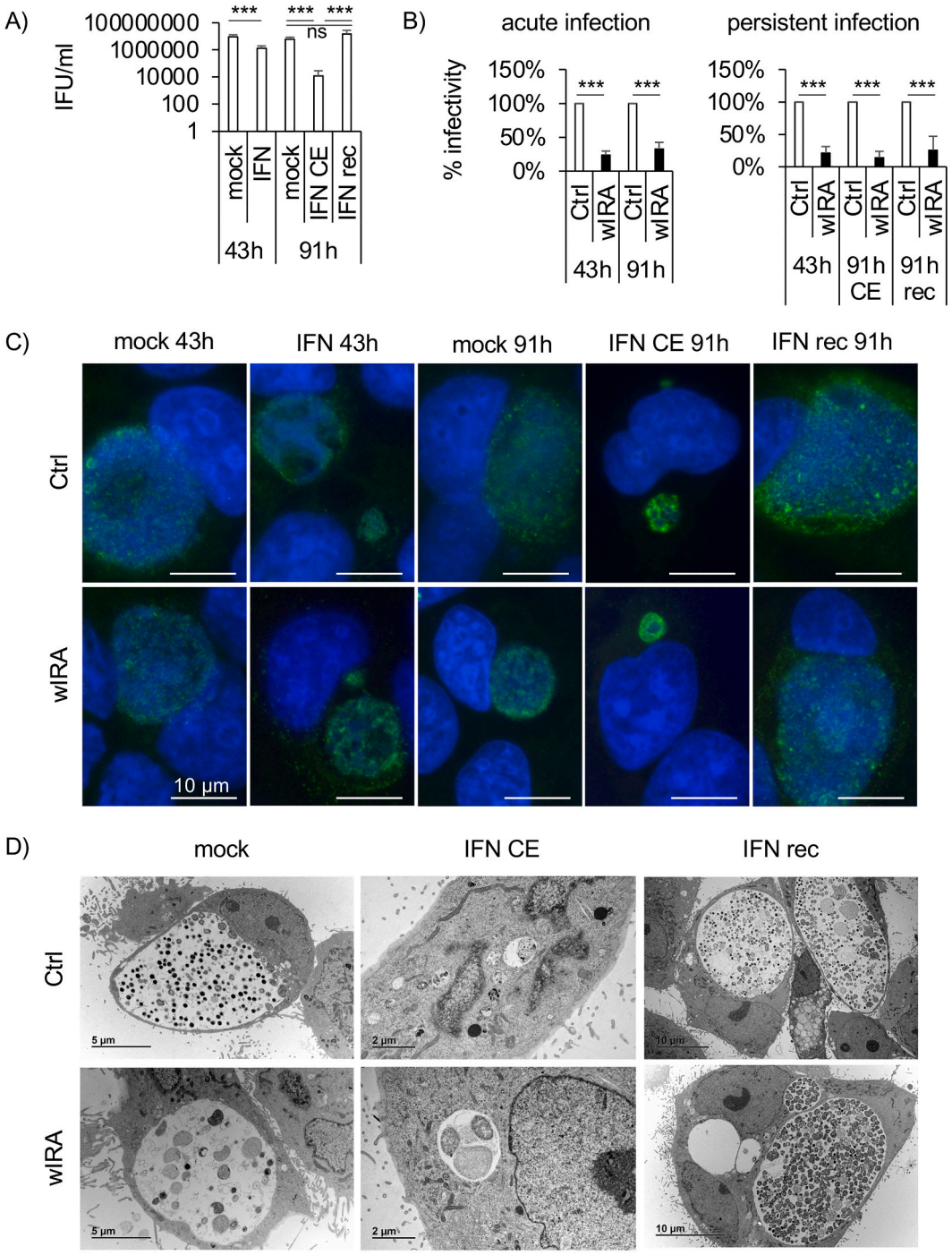

Fig. 5. Effects of IFN-γ and/or irradiation on chlamydial infectivity and morphology in a genital infection model: A) infectivity (IFU/ml) in non-irradiated conditions, exposed (IFN) or not (mock) to IFN-γ, and B) infectivity in non-irradiated controls (set to 100%) vs. wIRA and VIS treated conditions (expressed as % of control) for acute infection (exposed to diluent only, mock) and persistent infection (exposed to IFN). C) Representative immunofluorescence images of inclusions. D) Representative transmission electron microscopy images of inclusion ultrastructure at 91 hpi. For all plots, the bars represent values from three independent experiments ± SD. Statistical analysis was performed using a generalized linear model with IFU/ml raw data as response variables and experimental group (43 h mock vs. IFN, 91 h mock vs. IFN CE vs. IFN rec) and irradiation status (Ctrl vs. "wIRA") as explanatory factors. No interaction was detected for the applied model. Post hoc analysis was done with the Tukey test. *** $p < 0.001$.

explanations for this observation. It might be that chlamydial inclusions are variably susceptible for wIRA and VIS effects at different time points during their development. This hypothesis is supported by our observation that, for the higher irradiance (300 mW/cm^2), a single 15 min irradiation at 24 hpi significantly reduced chlamydial infectivity (resulting in a radiant exposure of 270 J/cm^2), while irradiation at the 36 and 40 hpi time points did not elicit a similar effect. In summary, additional studies are needed to investigate the variable susceptibility of chlamydial inclusions to wIRA and VIS irradiation at different time points during the developmental cycle. For future applications of wIRA *in vivo*, shorter irradiation durations would still be beneficial and antichlamydial effects might be enhanced by an aPDT approach, which is currently under our investigation.

Table 3
Interferon-γ and irradiation effects on chlamydial infectivity in the genital infection model with or without interferon-γ -induced persistence.

Sampling timepoint	Condition	Control only IFU/ml; Fig. 5A - IFN-γ effect	% of control after irradiation; Fig. 5B – irradiation effect
43 h	Mock	$8.94 \times 10^6 \pm 4.02 \times 10^6$	23.72 ± 5.93
	IFN-γ	$1.27 \times 10^6 \pm 7.05 \times 10^5$	21.10 ± 10.14
91 h	Mock	$6.15 \times 10^6 \pm 2.54 \times 10^6$	32.66 ± 9.81
	IFN-γ CE	$1.21 \times 10^4 \pm 1.70 \times 10^4$	13.87 ± 9.90
	IFN-γ rec	$1.46 \times 10^7 \pm 1.34 \times 10^7$	25.35 ± 21.70

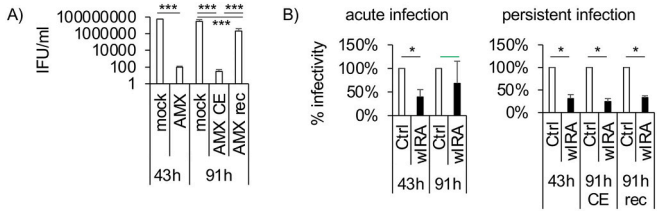

Fig. 6. Effects of AMX and/or irradiation on chlamydial infectivity in CtB-infected HeLa cells: A) infectivity (IFU/ml) in non-irradiated conditions, exposed (AMX) or not (mock) to amoxicillin, and B) infectivity in non-irradiated controls (set to 100%) vs. wIRA and VIS treated conditions (expressed as % of control) for acute infection (exposed to diluent only, mock) and persistent infection (exposed to AMX). For all plots, the bars represent values from three independent experiments ± SD. Statistical analysis was performed using a generalized linear model with IFU/ml raw data as response variables and experimental group (43 h mock vs. AMX, 91 h mock vs. AMX CE vs. AMX rec) and irradiation status (Ctrl vs. "wIRA") as explanatory variables. A significant interaction was detected between the acute infection 91 h and irradiation ("wIRA") group variable, as indicated in the plot by a green line. Significance levels: * $p < 0.05$, *** $p < 0.001$. (For interpretation of the references to colour in this figure legend, the reader is referred to the web version of this article.)

Table 4
Amoxicillin and irradiation effects on CtB infectivity in HeLa cells with or without amoxicillin-induced persistence.

Sampling timepoint	Condition	Control only IFU/ml; Fig. 6A - AMX effect	% of control after irradiation; Fig. 6B – irradiation effect	Comment
43 h	Mock	$5.44 \times 10^7 \pm 5.20 \times 10^6$	39.62 ± 15.42	
	AMX	$9.48 \times 10^1 \pm 3.27 \times 10^1$	31.11 ± 8.54	
91 h	Mock	$2.87 \times 10^7 \pm 1.86 \times 10^7$	68.54 ± 46.83	Interaction in GLM
	AMX CE	$3.06 \times 10^1 \pm 1.85 \times 10^1$	23.98 ± 6.76	
	AMX rec	$2.12 \times 10^6 \pm 1.84 \times 10^6$	32.71 ± 4.32	60 h recovery

4.3. The Chlamydial Stress Reponse In Vitro and Its Potential Clinical Relevance

While all our previous studies focused on acute chlamydial infection models (reviewed in [18–20]), wIRA and VIS effects on persistent chlamydial developmental stages have not been investigated to date. There are numerous stressors described that can cause chlamydial persistence (reviewed in [9,13,40,41]), but β-lactam antibiotics, interferon-gamma (IFN-γ) induced tryptophan (TRP) deprivation and iron chelators are considered the most clinically relevant persistence inducers [42]. We focused on the first two, since both are frequently studied and representative of two possible scenarios in actively infected trachoma patients (e.g. treatment with β-lactam antibiotics [43] or IFN-γ secretion in tear fluid [44,45]). β-lactam antibiotics block the peptidoglycan biosynthesis pathway present in *Chlamydia*, which is considered to be the mechanism by which they cause chlamydial persistence [13,46]. IFN-γ, a factor of the innate immune system, causes chlamydial aberrance in human culture models by reducing intracellular TRP availability via activation of the indoleamine 2,3-dioxygenase (IDO) [13,32,44]. In our experiments, we observed the previously described effects of β-lactam antibiotics (represented by AMX) such as the typical changes in chlamydial morphology and massive reduction of chlamydial infectivity, followed by recovery upon removal of antibiotics [13,42,46,47]. For IFN-γ we only observed mild effects at 43 hpi, however, we observed typical morphological changes and reduced infectivity at 91 hpi and a robust recovery upon removal of IFN-γ and supplementation of extracellular TRP which is in line with previously published studies [32,42,48]. In TEM analyses of IFN-exposed cultures, single aberrant bodies were observed, that did not exceed the size of 2 μm, which was also observed by others [42]. IFN-γ treatment of *Chlamydia* infected cells can cause cytotoxicity [32,49], as we noted it in our direct IFA analysis. Different consequences for bacterial/cellular pathways upon different persistence inducers are described, suggesting that persistence enables *Chlamydia* to survive in the presence of these various stress factors [13]. Generally, persistence induction pauses the chlamydial developmental cycle [13], which may be explained by type 3 secretion system (T3SS) dysfunction and subsequent blocked secretion of bacterial effector proteins [42]. Furthermore, different persistence inducers block secretion of different effector proteins, as demonstrated by Brockett and Liechti [42] or reviewed in [13]. In the context of the chlamydial developmental cycle, chlamydial survival is best supported when persistence is induced at an early time point after *Chlamydia* had overcome initial host cell intracellular defenses, but before an innate immune response is initiated, for example between 4 and 12 hpi for a *C. trachomatis* L2 strain [42].

4.4. Irradiation Efficacy Against Chlamydial Persistent Chlamydia – New Insights into Unresolved wIRA and VIS Anti-Chlamydial Working Mechanisms

Interestingly, we observed reductions of chlamydial infectivity upon irradiation independent from the experimental setting (chlamydial strain, cell type and irradiated chlamydial development form). This strongly suggests that wIRA and VIS effects are independent from the chlamydial developmental form and metabolism, and indicate that a general mechanism, not targeted to specific chlamydial structures or effectors, must be involved in wIRA and VIS anti-chlamydial effects. Surprisingly, we observed reproducible reductions in chlamydial infectivity independent of the persistence model, and specifically its effect on host cells, indicating that host cell metabolic status and secreted factors, if relevant, may only play a contributory role in anti-chlamydial irradiation effects. This conclusion is further supported by our observation that wIRA and VIS effects were maintained in cultures recovering from IFN-γ-induced persistence, even though additional TRP as extracellular nutrient was added to cultures. In previous mechanistic investigations, wIRA and VIS effects on chlamydial infectivity were found to be independent on host cytokine secretion such as IL-6, IL-8 and RANTES [29], which is in line with the sustained irradiation effects in the presence or absence of IFN-γ that we observed in this study.

In the 91 hpi mock condition (acute infection, recovery) in CtB infected HeLa cells, we did not consistently observe wIRA and VIS anti-chlamydial effects. We speculate that this variability could be caused by the high load of *Chlamydia* in this experimental condition, as the experiment used a high MOI (MOI = 10) due to the low infectivity of the

strain. We did not observe irradiation effects to be dependent on chlamydial MOI in previous investigations [27], however, an MOI as high as 10 over a long incubation time of 91 hpi has not been tested before. The high chlamydial infectious load might therefore have overwhelmed the efficacy of the anti-chlamydial effect of wIRA and VIS.

Interestingly, irradiation of persistent chlamydial stages sustained reduced infectivity, even after additional recovery times of 48 or 60 h, indicating that anti-chlamydial effects are maintained for at least one round of the developmental cycle. In a guinea pig model of acute ocular infection, a single exposure (595–1400 nm) reduced chlamydial infectious loads at 2, 4, 7 and 14 days post irradiation [20] also indicating a long-term irradiation effect. Further *in vivo* studies are needed to investigate whether chronic/persistent chlamydial infections can also be reduced by wIRA (and VIS) treatment *in vivo*.

4.5. Previously Reported Anti-Chlamydial Irradiations Effects

In this study, a broad wavelength spectrum (380–1400 nm) was used to treat aberrant chlamydial stages. Another study examined anti-chlamydial effects of 405 nm or 670 nm irradiations originating from light emitting diodes (LEDs) and the authors observed retarded chlamydial growth in unexposed control or penicillin-exposed cultures upon irradiation with 405 nm, but not 670 nm. However, the effect of wavelength on anti-chlamydial efficacy was not further commented on by the authors [50]. In our previous investigations, we evaluated either the efficacy of combined visible light and wIRA spectrum (termed wIRA/VIS, [26,29]) or more targeted wavelengths combinations using different filters and reducing the spectrum to 595–1400 nm (BTE595 orange filter) or 780–1400 nm (wIRA only, RG780 black filter) [20,21,27,28]. We observed similar anti-chlamydial efficacy for the filtered spectra excluding wavelengths below 595 nm as in the full spectrum, which partially contradicts the data of Wasson et al. [50]. However, technical differences in irradiation procedures and read-outs between these studies limit direct comparison.

4.6. Challenges in Identifying Anti-Chlamydial Working Mechanisms of wIRA and VIS

Several studies aimed to elucidate the working mechanism of wIRA (and VIS) against *Chlamydia*. These studies are reviewed and discussed elsewhere [18,19,51], while the following paragraph outlines remaining knowledge gaps. Previous investigations identified several factors affecting wIRA and VIS mediated anti-chlamydial activity, for example the wavelength spectrum of irradiation (more or less VIS (section 4.5)) or the involvement of thermal and non-thermal effects [27]. While single irradiations of either chlamydial EBs or host cells reduced subsequent chlamydial infectivity, irradiation of both EBs and host cells showed additive anti-chlamydial effects, which indicated an involvement of cellular and bacterial factors in the working mechanism [28]. However, host cell cytokine induction as a main mechanism was not evident in previous studies [27,29]. Interestingly, anti-EB effects of irradiation were dependent on irradiance (higher irradiance leading to stronger effects), which was not the case in irradiation of growing chlamydial inclusions [27], which is in line with our observation that irradiances of 150 and 200 mW/cm^2 had similar effects on infectivity (section 3.6). In contrast to the previous results with 1 × 20 min wIRA and VIS irradiation at 40 hpi [27], however, we did not observe a significant reduction of chlamydial infectivity at 100 mW/cm^2, even though we performed triple irradiations of developing inclusions. This discrepancy may be explained by differences in statistical analyses or the higher standard deviation for our experimental data compared to the previous study. Despite these incongruities, we can conclude from our current and previous experimental data that higher irradiances are more effective against extracellular, infectious chlamydial particles (EBs, important in the context of transmission control). In contrast, for developing chlamydial inclusions, irradiances at 150 or 200 mW/cm^2 provide similar anti-chlamydial effects as levels >200 mW/cm^2. Even though previously no harmful effects have been reported even at higher irradiances (210 mW/cm^2*in vivo* [21], 370 mW/cm^2*in vitro* [26]) an irradiance of 150–200 mW/cm^2 is recommended for use in future safety studies *in vivo* as increased heat is correlated with increased irradiances [28]. Other applications of low-level light sources for medical use are referred to by the terms “photobiomodulation” or “low-level light therapy (LLLT)” [52]. Typical biological effects for these treatment modalities are reactive oxygen species (ROS)-release and the typically bi-phasic response which shows beneficial biological effects at low irradiation levels, but detrimental effects at higher fluences [53,54]. The application of infrared irradiation for the skin is considered safe in the tenths of J/cm^2, while fluences in the range of hundreds of J/cm^2 are considered harmful, inducing skin hyperthermia and associated inductions of deleterious pathways [53].

Interestingly, this and previous investigations did not confirm consistent detrimental effects of wIRA (and VIS) on host cells and/or host tissues, even at high irradiances and/or long irradiation durations [21,26,28]. While biological effects of infrared A in mammalian cells are likely induced upon absorption of light energy by photoacceptor molecules like the cytochrome *c* oxidase, such photoacceptor homologues, to our knowledge, are not reported in *Chlamydia*. However, Chlamydiae as obligate intracellular bacteria are widely dependent on factors originating from host cells [55]. Evolutionarily, these bacteria have reduced genomes and subsequent protein translation, but nonetheless are master regulators of cellular organelle structures and functions [1]. This inseparable relationship between *Chlamydia* and their host cells makes it difficult to distinguish bacteria-induced from irradiation-induced cellular changes and even more difficult to identify direct anti-chlamydial effects, as any impact on bacterial development must be analyzed in the context of the host cell system.

4.7. Main Findings and Significance

We found wIRA and VIS to be effective even against persistent chlamydial stages that are considered more difficult to treat with standard antibiotic treatments [11,12]. The anti-chlamydial mechanism of this irradiation is likely independent from specific chlamydial effectors or structures, since it was consistently present in different cell culture models [26,28] using different chlamydial species [26], strains or persistence inducers. Such non-specific mechanisms, though challenging to identify and characterize, are less likely to induce bacterial mutations or progressive development of resistance (e.g. photodynamic treatments - [39]), which represent a significant advantage of wIRA irradiation compared to use of antibiotic treatment alone.

5. Outlook

We confirmed reliable and constant anti-chlamydial efficacy of wIRA and VIS irradiation against two clinically relevant strains of *Chlamydia trachomatis* (CtE and CtB) using two different *in vitro* models of chlamydial persistence to simulate chronic infections in human patients. Our investigation of potential refinement of applications of wIRA and VIS showed that a minimal thresholds of exposure time (between 30 and 45 min) and of irradiance (150 mW/cm^2) must be met to induce significant antibacterial activity. Single or double irradiation treatments of acute chlamydial infections *in vivo* for 30 min (595–1400 nm, 210 mW/cm^2) showed significant anti-chlamydial efficacy [20,21], which awaits confirmation in persistent chlamydial infection studies *in vivo*.

Investigation of wIRA (and VIS) irradiation as a light source in a combined anti-chlamydial aPDT setting is currently ongoing and will provide further information for enhancement studies *in vitro* and *in vivo*. These investigations should be followed by *in vivo* safety studies focusing on the above-mentioned parameters of irradiation time and doses to ensure safe and tolerable use of wIRA irradiation in human trachoma patients.

Supplementary data to this article can be found online at https://doi.org/10.1016/j.jphotobiol.2022.112533.

Funding

This work was supported by the Dr. med. h.c. Erwin Braun Foundation, Basel, Switzerland.

Declaration of Competing Interest

The authors declare that they don't have any conflict of interests.

Acknowledgments

We thank Lisbeth Nufer for her help with transmission electron microscopy pictures and Prof. Dr. Paul Torgerson for his support regarding statistical analysis.

References

[1] C. Elwell, K. Mirrashidi, J. Engel, Chlamydia cell biology and pathogenesis, Nat. Rev. Microbiol. 14 (2016) 385–400, https://doi.org/10.1038/nrmicro.2016.30.
[2] M. Wolle, S. West, Ocular Chlamydia trachomatis infection: elimination with mass drug administration, Expert Rev. Anti-Infect. Ther. 17 (2019) 189–200, https://doi.org/10.1080/14787210.1577136.
[3] H.R. Taylor, M.J. Burton, D. Haddad, S. West, H. Wright, Trachoma, Lancet. 384 (2014) 2142–2152, https://doi.org/10.1016/S0140-6736(13)62182-0.
[4] WHO, WHO Trachoma. https://www.who.int/news-room/fact-sheets/detail/trachoma, 2022.
[5] S.K. West, Milestones in the fight to eliminate trachoma, Ophthalmic Physiol. Opt. 40 (2020) 66–74, https://doi.org/10.1111/opo.12666.
[6] WHO, Weekly Epidemiological Record. https://www.who.int/publications/journals/weekly-epidemiological-record, 2020.
[7] G. Satpathy, H. Behera, N. Ahmed, Chlamydial eye infections: current perspectives, Indian J. Ophthalmol. 65 (2017) 97–102, https://doi.org/10.4103/ijo.IJO_870_16.
[8] N. Borel, C. Leonard, J. Slade, R.V. Schoborg, Chlamydial antibiotic resistance and treatment failure in veterinary and human medicine, Curr. Clin. Microbiol. Reports. 3 (2016) 10–18, https://doi.org/10.1007/s40588-016-0028-4.
[9] P.B. Wyrick, Chlamydia trachomatis persistence in vitro: an overview, J. Infect. Dis. 201 (2010) 88–95, https://doi.org/10.1086/652394.
[10] P.M. Bavoil, What's in a word: the use, misuse, and abuse of the word " persistence" in Chlamydia biology, Front. Cell. Infect. Microbiol. 4 (2014), https://doi.org/10.3389/fcimb.2014.00027.
[11] P.B. Wyrick, S.T. Knight, Pre-exposure of infected human endometrial epithelial cells to penicillin in vitro renders Chlamydia trachomatis refractory to azithromycin, J. Antimicrob. Chemother. 54 (2004) 79–85, https://doi.org/10.1093/jac/dkh283.
[12] R. Phillips-Campbell, J. Kintner, R.V. Schoborg, Induction of the Chlamydia muridarum stress/persistence response increases azithromycin treatment failure in a murine model of infection, Antimicrob. Agents Chemother. 58 (2014) 1782–1784, https://doi.org/10.1128/AAC.02097-13.
[13] M.E. Panzetta, R.H. Valdivia, H.A. Saka, Chlamydia persistence: a survival strategy to evade antimicrobial effects in-vitro and in-vivo, Front. Microbiol. 9 (2018) 1–11, https://doi.org/10.3389/fmicb.2018.03101.
[14] G. Hoffmann, Water-filtered infrared-A (wIRA) in acute and chronic wounds, GMS Krankenhhyg, Interdiszip. 4 (2009).
[15] H. Piazena, W. Müller, W. Pendl, S. von Ah, V.H. Cap, P.J. Hug, X. Sidler, G. Pluschke, P. Vaupel, Thermal field formation during wIRA-hyperthermia: temperature measurements in skin and subcutis of piglets as a basis for thermotherapy of superficial tumors and local skin infections caused by thermosensitive microbial pathogens, Int. J. Hyperth. 36 (2019) 937–952, https://doi.org/10.1080/02656736.2019.1655594.
[16] H. Piazena, H. Meffert, R. Uebelhack, Spectral remittance and transmittance of visible and infrared-A radiation in human skin—comparison between in vivo measurements and model calculations, Photochem. Photobiol. (2017), https://doi.org/10.1111/php.12785.
[17] H. Piazena, W. Müller, P. Vaupel, Physical and photobiological basics of wIRA-Hyperthermia, in: P. Vaupel (Ed.), Water-Filtered Infrared A Irradiat. - From Res. to Clin. Settings, 1st ed., Springer Nature Switzerland AG, 2022, pp. 35–54, https://doi.org/10.1007/978-3-030-92880-3_3.
[18] J. Kuratli, N. Borel, Perspective: water-filtered infrared-a-radiation (WIRA) - novel treatment options for chlamydial infections? Front. Microbiol. 10 (2019) https://doi.org/10.3389/fmicb.2019.01053.
[19] N. Borel, A.M. Sauer-Durand, M. Hartel, J. Kuratli, P. Vaupel, N. Scherr, G. Pluschke, wIRA: hyperthermia as a treatment option for intracellular bacteria, with special focus on Chlamydiae and mycobacteria, Int. J. Hyperth. 37 (2020) 373–383, https://doi.org/10.1080/02656736.2020.1751312.
[20] A. Inic-Kanada, M. Stojanovic, R. Miljkovic, E. Stein, A. Filipovic, A. Frohns, N. Zöller, J. Kuratli, T. Barisani-Asenbauer, N. Borel, Water-filtered infrared A and visible light (wIRA/VIS) treatment reduces Chlamydia caviae-induced ocular inflammation and infectious load in a Guinea pig model of inclusion conjunctivitis, J. Photochem. Photobiol. B Biol. 209 (2020), 111953, https://doi.org/10.1016/j.jphotobiol.2020.111953.
[21] A. Frohns, M. Stojanovic, T. Barisani-Asenbauer, J. Kuratli, N. Borel, A. Inic-Kanada, Effects of water-filtered infrared A and visible light (wIRA/VIS) radiation on heat- and stress-responsive proteins in the retina and cornea of guinea pigs, J. Photochem. Photobiol. B Biol. 224 (2021), https://doi.org/10.1016/j.jphotobiol.2021.112306.
[22] S.M. Garland, A. Malatt, S. Tabrizi, D. Grando, M.I. Lees, J.H. Andrew, H.R. Taylor, Chlamydia trachomatis conjunctivitis: prevalence and association with genital tract infection, Med. J. Aust. 162 (1995) 363–366, https://doi.org/10.5694/j.1326-5377.1995.tb139939.x.
[23] E.J. Postema, L. Remeijer, W.I. Van Der Meijden, Epidemiology of genital chlamydial infections in patients with chlamydial conjunctivitis; a retrospective study, Genitourin. Med. 72 (1996) 203–205.
[24] K. Mohamed-Noriega, J. Mohamed-Noriega, M.A. Valdés-Navarro, E.E. Cuervo-Lozano, M.C. Fernández-Espinosa, J. Mohamed-Hamsho, Conjunctival infection with Chlamydia trachomatis in sexual partners of patients with adult inclusion conjunctivitis, Int. Ophthalmol. 35 (2015) 179–185, https://doi.org/10.1007/s10792-014-9930-z.
[25] W.J.A. Lee, C.C. Chen, Adult inclusion conjunctivitis diagnosed by polymerase chain reaction and Giemsa stain, IDCases. 27 (2022), e01367, https://doi.org/10.1016/j.idcr.2021.e01367.
[26] H. Marti, M. Koschwanez, T. Pesch, C. Blenn, N. Borel, Water-filtered infrared a irradiation in combination with visible light inhibits acute chlamydial infection, PLoS One 9 (2014), https://doi.org/10.1371/journal.pone.0102239.
[27] H. Marti, C. Blenn, N. Borel, The contribution of temperature, exposure intensity and visible light to the inhibitory effect of irradiation on acute chlamydial infection, J. Photochem. Photobiol. B Biol. 153 (2015) 324–333, https://doi.org/10.1016/j.jphotobiol.2015.10.012.
[28] C. Rahn, H. Marti, A. Frohns, F. Frohns, C. Blenn, C.A. Leonard, T. Barisani-Asenbauer, E. Stein, N. Borel, Water-filtered infrared A reduces chlamydial infectivity in vitro without causing ex vivo eye damage in pig and mouse models, J. Photochem. Photobiol. B Biol. 165 (2016) 340–350, https://doi.org/10.1016/j.jphotobiol.2016.11.001.
[29] J. Kuratli, T. Pesch, H. Marti, C.A. Leonard, C. Blenn, P. Torgerson, N. Borel, Water filtered infrared a and visible light (wIRA/VIS) irradiation reduces chlamydia trachomatis infectivity independent of targeted cytokine inhibition, Front. Microbiol. 9 (2018) 1–14, https://doi.org/10.3389/fmicb.2018.02757.
[30] C.A. Leonard, R.V. Schoborg, N. Borel, Damage/danger associated molecular patterns (DAMPs) modulate chlamydia pecorum and C. trachomatis serovar e inclusion development in vitro, PLoS One 10 (2015), https://doi.org/10.1371/journal.pone.0134943.
[31] I. Miyairi, O.S. Mahdi, S.P. Ouellette, R.J. Belland, G.I. Byrne, Different growth rates of Chlamydia trachomatis biovars reflect pathotype, J. Infect. Dis. 194 (2006) 350–357, https://doi.org/10.1086/505432.
[32] W.L. Beatty, T.A. Belanger, A.A. Desai, R.P. Morrison, G.I. Byrne, Tryptophan depletion as a mechanism of gamma interferon- mediated chlamydial persistence, Infect. Immun. 62 (1994) 3705–3711.
[33] J. Kuratli, C.A. Leonard, L. Nufer, H. Marti, R. Schoborg, B. Nicole, Maraviroc, celastrol and azelastine alter Chlamydia trachomatis development in HeLa cells, J. Med. Microbiol. 69 (2020) 1351–1366, https://doi.org/10.1099/jmm.0.001267.
[34] E. Staub, H. Marti, R. Biondi, A. Levi, M. Donati, C.A. Leonard, S.D. Ley, T. Pillonel, G. Greub, H.M.B. Seth-Smith, N. Borel, Novel Chlamydia species isolated from snakes are temperature-sensitive and exhibit decreased susceptibility to azithromycin, Sci. Rep. 8 (2018), https://doi.org/10.1038/s41598-018-23897-z.
[35] D. Onorini, M. Donati, H. Marti, R. Biondi, A. Levi, L. Nufer, B. Prähauser, S. Rigamonti, N. Vicari, N. Borel, The influence of centrifugation and incubation temperatures on various veterinary and human chlamydial species, Vet. Microbiol. 233 (2019) 11–20, https://doi.org/10.1016/j.vetmic.2019.04.012.
[36] T. Hothorn, F. Bretz, P. Westfall, Simultaneous inference in general parametric models, Biom. J. 50 (2008) 346–363, https://doi.org/10.1002/bimj.200810425.
[37] J.S. Zigler, J.L. Lepe-Zuniga, B. Vistica, I. Gery, Analysis of the cytotoxic effects of light-exposed hepes-containing culture medium, Vitr. Cell. Dev. Biol. 21 (1985) 282–287, https://doi.org/10.1007/BF02620943.
[38] R.S. Rubinfeld, C. Caruso, C. Ostacolo, Corneal cross-linking: the science beyond the myths and misconceptions, Cornea. 38 (2019) 780–790, https://doi.org/10.1097/ICO.0000000000001912.
[39] M.R. Hamblin, T. Hasan, Photodynamic therapy: a new antimicrobial approach to infectious disease? Photochem. Photobiol. Sci. 3 (2004) 436–450, https://doi.org/10.1039/b311900a.
[40] R.J. Hogan, S.A. Mathews, S. Mukhopadhyay, J.T. Summersgill, P. Timms, Chlamydial persistence: beyond the biphasic paradigm, Infect. Immun. 72 (2004) 1843–1855, https://doi.org/10.1128/IAI.72.4.1843-1855.2004.
[41] R.V. Schoborg, Chlamydia persistence - a tool to dissect chlamydia-host interactions, Microbes Infect. 13 (2011) 649–662, https://doi.org/10.1016/j.micinf.2011.03.004.
[42] M.R. Brockett, G.W. Liechti, Persistence alters the interaction between chlamydia trachomatis and its host cell, Infect. Immun. 89 (2021), https://doi.org/10.1128/IAI.00685-20.
[43] J. Kintner, D. Lajoie, J. Hall, J. Whittimore, R.V. Schoborg, Commonly prescribed β-lactam antibiotics induce c.trachomatis persistence/stress in culture at physiologically relevant concentrations, Front. Cell. Infect. Microbiol. 4 (2014) 1–10, https://doi.org/10.3389/fcimb.2014.00044.

[44] P.A. Rapoza, G.T. Sjakon, J.P. Carlin, S.L. Miller, M.L. Padilla, G.I. Byrne, Effect of interferon on a primary conjunctival epithelial cell model of trachoma, Investig. Ophthalmol. Vis. Sci. 32 (1991) 2919–2923.
[45] L. Bobo, N. Novak, H. Mkocha, S. Vitale, S. West, T.C. Quinn, Evidence for a predominant proinflammatory conjunctival cytokine response in individuals with trachoma, Infect. Immun. 64 (1996) 3273–3279, https://doi.org/10.1128/iai.64.8.3273-3279.1996.
[46] N. Jacquier, P.H. Viollier, G. Greub, The role of peptidoglycan in chlamydial cell division: towards resolving the chlamydial anomaly, FEMS Microbiol. Rev. 39 (2015) 262–275, https://doi.org/10.1093/femsre/fuv001.
[47] M. Matsumoto, K. Funami, H. Oshiumi, T. Seya, Toll-like receptor 3: a link between toll-like receptor, interferon and viruses, Microbiol. Immunol. 48 (2004) 147–154, https://doi.org/10.1111/j.1348-0421.2004.tb03500.x.
[48] W.L. Beatty, G.I. Byrne, R.P. Morrison, Morphologic and antigenic characterization of interferon γ-mediated persistet Chlamydia trachomatis infection in vitro, Proc. Natl. Acad. Sci. U. S. A. 90 (1993) 3998–4002.
[49] G.I. Byrne, C.S. Schobert, D.M. Williams, D.A. Krueger, Characterization of gamma interferon-mediated cytotoxicity to chlamydia-infected fibroblasts, Infect. Immun. 57 (1989) 870–874, https://doi.org/10.1128/iai.57.3.870-874.1989.
[50] C.J. Wasson, J.L. Zourelias, N.A. Aardsma, J.T. Eells, M.T. Ganger, J.M. Schober, T. A. Skwor, Inhibitory effects of 405nm irradiation on Chlamydia trachomatis growth and characterization of the ensuing inflammatory response in HeLa cells, BMC Microbiol. 12 (2012), https://doi.org/10.1186/1471-2180-12-176.
[51] J. Kuratli, H. Marti, C. Blenn, N. Borel, Water-filtered infrared A (wIRA) irradiation: novel treatment options for chlamydial infections, in: P. Vaupel (Ed.), Water-Filtered Infrared A Irradiat. - From Res. to Clin. Settings, 1st ed., Springer Nature Switzerland AG, 2022, pp. 247–258, https://doi.org/10.1007/978-3-030-92880-3.
[52] M.R. Hamblin, Y.-Y. Huang, V. Heiskanen, Non-mammalian hosts and photobiomodulation: do all life-forms respond to light? Photochem. Photobiol. 95 (2019) 126–139, https://doi.org/10.1111/php.12951.
[53] D. Barolet, F. Christiaens, M.R. Hamblin, Infrared and skin: Friend or foe, J. Photochem. Photobiol. B Biol. (2016), https://doi.org/10.1016/j.jphotobiol.2015.12.014.
[54] S.-R. Tsai, M.R. Hamblin, Biological effects and medical applications of infrared radiation, J. Photochem. Photobiol. B Biol. 170 (2017) 197–207, https://doi.org/10.1016/j.jphotobiol.2017.04.014.
[55] C. Sütterlin, I. Derré, Interaction of the chlamydial inclusion with the host cell, in: M. Tan, J.H. Hegemann, C. Sütterlin (Eds.), Chlamydia Biol. From Genome to Dis, 1st ed, Caister Academic Press, Norfolk, UK, 2020, pp. 111–134, https://doi.org/10.21775/9781912530281.05.